ELSEVIER

Journal of Organometallic Chemistry 641 (2002) 227–234

Journal of Organometallic Chemistry

www.elsevier.com/locate/jorganchem

Strain in organometallics: synthesis of rhodium and iridium complexes with a novel rigid tetrachelating phosphine olefin ligand and their redox properties

Cécile Laporte, Carsten Böhler, Hartmut Schönberg, Hansjörg Grützmacher *

Laboratory of Inorganic Chemistry, Department of Chemistry, ETH-Hönggerberg, CH-8093 Zurich, Switzerland

Received 24 September 2001

Dedicated to Professor Rolf Gleiter on the occasion of his 65th birthday

Abstract

The new tetrachelating diphosphanes 1,2-[(5*H*-dibenzo[a,d]cyclohepten-5-yl)phenylphosphano]ethane, *R*,*S*-**11** [*R*,*S*-bis(tropp^{Ph})], and the corresponding enantiomers *R*,*R*-bis(tropp^{Ph}), *R*,*R*-**12**, and *S*,*S*-bis(tropp^{Ph}), *S*,*S*-**12**, were synthesised from 1,2-bis(phenylphosphano)ethane (**9**), and 5-chloro-5*H*-dibenzo[a,d]cycloheptene (**10**). With the *meso* form *R*,*S*-**11**, the rhodium(I) complex [Rh{*R*,*S*-bis(tropp^{Ph})}]PF_6 (**15**), and the iridium(I) complex [Ir(cod){*R*,*S*-bis(tropp^{Ph})}]O_3SCF_3 (**16**), were prepared. The cation of the 16-electron rhodium complex **15** has a square planar structure, which is markedly distorted towards a square pyramid with the rhodium centre in the apex. The structure of the cation of the 18-electron complex of **16** is trigonal bipyramidal and unprecedented a phosphorus and an olefin unit occupy the axial positions. Cyclic voltammetry data of **15** indicate, that considerable strain energy (ca. 30 kJ mol^{-1}) is build up when the [Rh{*R*,*S*-bis(tropp^{Ph})}]$^+$ cation is reversibly reduced in THF by one electron to the paramagnetic neutral complex [Rh{*R*,*S*-bis(tropp^{Ph})}]^0. © 2002 Published by Elsevier Science B.V.

Keywords: Cyclic voltammetry; Iridium; Phosphanes; Rhodium; Redox chemistry; Strain energy

1. Introduction

We developed the synthesis of the ^{R1}tropp^{R} ligand system (tropp = tropylidene phosphane; IUPAC 5-diphenylphosphanyl-dibenzo[a,d]cycloheptene; R indicates the substituent bonded to the phosphorus, R^1 the substituent bonded to the central olefinic unit) which contains a seven-membered ring in a rigid boat conformation such that a phosphanyl and olefinic binding site are optimally placed to co-ordinate with various metals (Scheme 1) [1].

It turned out that the 16-electron *trans*- and *cis*-[M(tropp^{ph})$_2$]$^+$ cations **1**, **2** (M = Rh, Ir) containing the P–phenyl substituted ligand tropp^{ph} are reversibly reduced in two successive single electron transfer steps at remarkably low negative potentials [2,3]. All complexes shown in Scheme 1 were isolated and fully characterised. By NMR and EPR spectroscopic studies, it was shown that the diamagnetic complexes **1**, **2**, **5** and **6** are stereochemically rigid, i.e. the 16-electron complex cations **1** and **2** exist as mixture of *trans*- and *cis*-isomers which do not inter-convert in weakly co-ordinating solvents on the NMR time scale and the 18-electron metalates **5** and **6** exist *cis*-isomers exclusively. On the other hand, the paramagnetic 17-electron complexes **3** and **4** are highly dynamic. The observed *trans*–*cis*-isomerisation proceeds most likely via an intra-molecular rotation of the tropp ligands [4]. In the solid state, all complexes in Scheme 1 show a square planar structure, which is severely distorted towards a tetrahedron. This distortion is defined by the intersection angle φ of the planes *p1* and *p2* running through the phosphorus atom, the centroid of the co-ordinated olefin indicated by black circles in Scheme 1 and the metal centre. In the 16-electron cations, φ lies in the range between 0 and 30° in *trans*-**1** depending on the counter anion. In

* Corresponding author. Tel.: +41-1-6322855; fax: +41-1-6321090.

E-mail address: gruetzmacher@inorg.chem.ethz.ch (H. Grützmacher).

0022-328X/02/$ - see front matter © 2002 Published by Elsevier Science B.V.
PII: S0022-328X(01)01362-6

the paramagnetic species **3** and **4**, φ values of 34 and 43° were observed and the d^{10} valence configurated metalates **5** and **6** show with $\varphi = 53-58°$ the strongest deviations.

A methyl substituent at the central C=C double bond was introduced and the complex **7** containing the $^{me}tropp^{ph}$ ligand [5] could be prepared. Steric interactions in **7**, which exists as *cis*-isomer exclusively, induce a severe distortion from a square planar towards a tetrahedral configuration ($\varphi = 42°$). Thereby, the ground state of the 16-electron cation—preferring a planar structure—should be destabilised with respect to the reduced forms and an even lower reduction potential should result. However, although examples for this approach are well documented [6–8], only very small effects on the redox potentials of **7** were established [5].

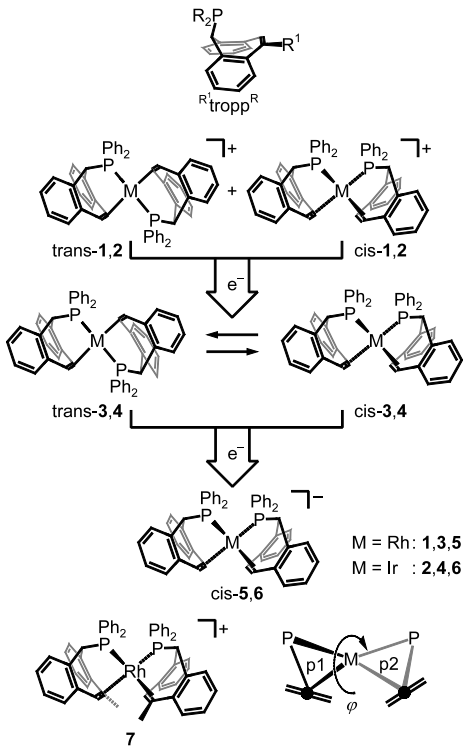

Scheme 1. Rhodium, **1**, **3**, **5**, **7** and iridium, **2**, **4**, **6**, $^{R1}tropp^{R}$ complexes.

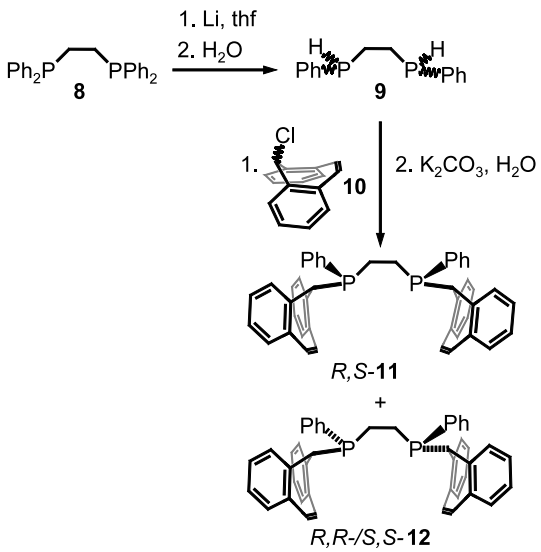

Scheme 2. Synthesis of the bis(tropp) ligands *R,S*-**11** and *R,R*-/*S,S*-**12**.

As a next step, we became interested in the influence of a chelating bi(tropp)–ligand system on the redox properties. Such a constraint in the ligand allows only *cis*-isomers to be formed and in general impedes the adoption of the coordination sphere to the formal oxidation state of the metal. We report here on the synthesis of such a ligand in which both phosphorus centres are covalently linked, the preparation of rhodium and iridium complexes and first studies concerning their redox properties.

2. Results and discussion

We chose a chelating tropp system derived from 1,2-bis-(phenylphosphano)ethane (dppe) (**8**) to start with. In this context we mention that the redox chemistry of the complexes $[M(dppe)_2]^+$ (M = Rh, Ir) has been intensively studied [9–12], the fluxionality of $[Rh(dppe)_2]^0$ [12,13] and the reactivity of $[Rh(dppe)_2]^-$ [14] has been investigated. Note, that high negative potentials must be employed (< -2 V) to generate the reduced species. According to a recently published procedure, the bis(phosphane) **8** can be easily converted into the secondary bis(phosphane) **9** by reductive cleavage of one P–phenyl bond on each phosphorus atom and subsequent hydrolysis of the intermediate bis(lithiophosphanyl)ethane [15] (Scheme 2).

Following a previously described protocol [1], reaction of **9** with 5-chloro-5*H*-dibenzo[a,d]cycloheptene (**10**) gives a mixture of 65% of the *meso* form, *R,S*-1,2-[(5*H*-dibenzo[a,d]cyclohepten-5-yl)diphenylphosphino]-ethane (**11**), and 35% of the racemate *R,R*-/*S,S*-**12** [16]. The total yield of both diastereomers amounts about 60%. Fortunately, the *meso* and the racemic forms **11** and **12**, respectively, could be easily separated by simple fractional crystallisation. From toluene, the *R,S*-**11** isomer crystallised first in spectroscopically pure form (^{31}P, $\delta = -16.52$) and after addition of acetonitrile the *R,R*-/*S,S*-**12** isomer (^{31}P, $\delta = -18.41$) crystallised in about 95% purity.

As the ^{31}P-NMR spectra showed, reactions with the mixture of the chiral bis(tropp) ligands *R,R*/*S,S*-**12** and various organometallic precursors of rhodium(I) and iridium(I) are rather complex and did not give the expected products. Only one product was obtained in

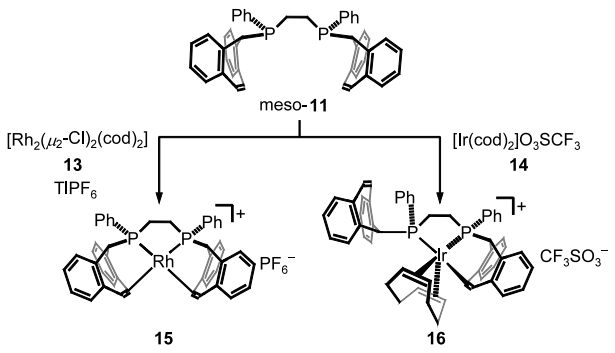

Scheme 3. Synthesis of rhodium(I) **15** and iridium(I) bis(tropp) complexes **16**.

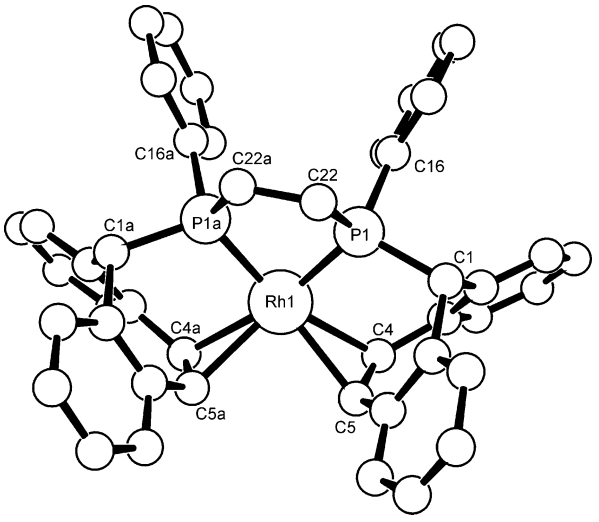

Fig. 1. Molecular structure of **15**. The PF_6 counter anion and the hydrogen atoms were omitted for clarity. Selected bond lengths and angles are given in Table 1.

good to excellent yields with the *meso*-isomer **11** when the dinuclear complex $[Rh_2(\mu_2\text{-}Cl)_2(cod)_2]$ **13** shown in Scheme 3, $TlPF_6$ and *R,S*-**11** are mixed in equimolar ratios in THF, the solution becomes deep red and the expected reaction product **15** is formed in 94% isolated yield.

The ^{31}P-NMR spectrum of a methylene chloride solution of **15** shows only one sharp doublet in the δ range typical for these of complexes ($\delta = 107.6$; $^1J_{RhP} = 177$ Hz) [2,5]. Concerning the binding of the olefinic units of the ligand, the ^{1}H-NMR spectrum is little informative, because, these protons are buried within the range of absorptions for the aromatic protons ($\delta = 6.67$–7.63). Noteworthy is the high frequency shift ($\delta = 2.40$) of one pair of the diastereotopic protons of the CH_2–CH_2-bridge (the other pair is observed at and $\delta = 1.52$) compared with the uncomplexed ligand (*R,S*-**11**: $\delta = 1.16$). In the ^{13}C-NMR spectrum, two multiplets centred $\delta = 97.5$ and 103.1 are assigned to the co-ordinated olefins; neither the ^{103}Rh^{13}C nor the ^{31}P^{13}C couplings were determined. The chemical shifts are typical for tropp complexes with a *cis* conformation [5,17] and are displaced by about $\Delta\delta = 25$ to lower frequencies when compared with the uncomplexed ligand *R,S*-**11** ($\delta = 127.7$ and another absorption $\delta > 127.9$ which could not be distinguished from the resonance signals of the aromatic carbon nuclei).

When $[Ir(cod)_2]O_3SCF_3$ **14** is mixed with bis(tropp) *R,S*-**11** in methylene chloride, an orange–yellow solution is obtained from which yellow crystals precipitated after adding *n*-hexane. The re-dissolved product **16**, as well as the reaction mixture, shows two sharp singlets in the ^{31}P-NMR spectrum ($\delta = 12.7$, 66.58) which is incompatible with the formation of a [Ir{bis(tropp)}] complex like **15**. The ^{1}H- and ^{13}C-NMR spectra are extremely complex (for that reason they are not reported here) and it was not possible to conclude from the spectral data on the structure of complex **16**. Varying the reaction conditions (i.e. longer reaction times, higher temperatures up to 120 °C, other solvents) or using $[Ir_2(\mu_2\text{-}Cl)_2(cod)_2]$ in presence of $TlPF_6$ also led to the formation of **16** which eventually decomposed under formation of elemental iridium under harsh reaction conditions.

3. Molecular structures of 15 and 16

Crystals of **15** and **16** suitable for X-ray analyses were grown by diffusion of *n*-hexane into concentrated methylene chloride solutions. The molecular structures of the cations of **15** and **16** are shown in Figs. 1 and 2 and selected bond lengths and angles are listed in Tables 1 and 2, respectively. Crystallographic data are compiled in Table 4, which is given in Section 5.

The steric stress imposed by the ligand system is clearly reflected in the structure of the rhodium(I) complex **15**. The centroids Ct1 and Ct1a of the co-ordinated olefin units C4=C5 and C4a=C5a, respectively, of each tropp ligand and the two phosphorus atoms P1 and P1a span a square planar co-ordination sphere around the metal centre which is distorted towards a square pyramid such that the Rh1 atom lies 0.278 Å above the P1, P1a, Ct1, Ct1a plane [see Fig. 1 and (a) on top of Scheme 4].

This type of distortion seems to be rare while tetrahedral distortions in d^8 metal valence electron configurated complexes are frequently observed [see (b) on top of Scheme 4 and Ref. [5]]. The latter distortion is obviously not possible for **15** due to the ethylene bridge. The C22–C22a single bond of this bridge is slightly compressed to 1.47(2) Å and the CH_2 units are located in an eclisped position (torsion angle P1a–C22a–C22–P1 = 10.1°) within the five membered RhP_2C_2 heterocycle which has an envelope conformation folded by 29° along the P1–P1a vector. Further-

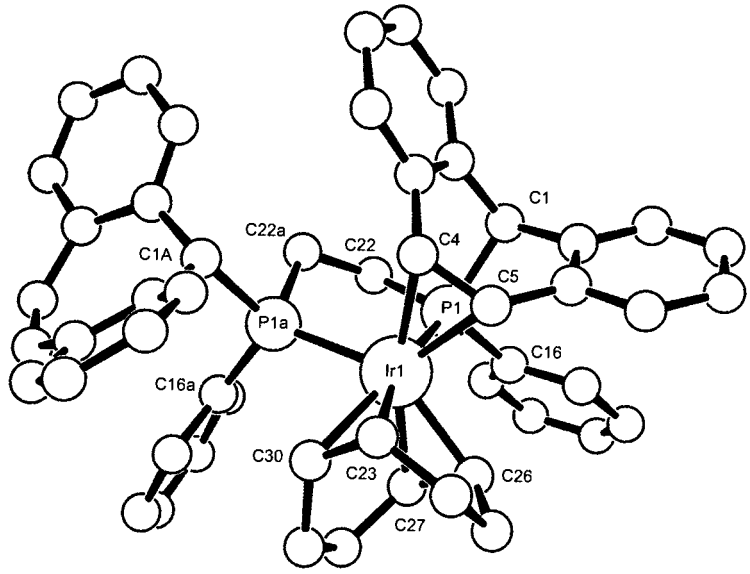

Fig. 2. Molecular structure of **16**. The CF_3SO_3 counter anion and the hydrogen atoms were omitted for clarity. Selected bond lengths and angles are given in Table 2.

more, the steric congestion in the complex cation of **15** is reflected by the relatively long Rh–C bonds [2.31(1)–2.36(1) Å; distances to the olefin centroids: Rh–Ct1 2.23 Å, Rh–Ct1a 2.21 Å], which are about 0.2 Å longer than usual Rh–C bond lengths in comparable compounds (ca. 2.15 Å) [18]. However, such long M–C bonds seem to be typical for *cis*-configurated [M(tropp)$_2$] complexes and even longer ones have been observed in **17** (Scheme 1) [5,17]. On the other hand, the rhodium phosphorus bonds [2.208(2), 2.227(2) Å] have normal lengths.

The structure of the iridium complex cation, [Ir(cod){*R*,*S*-bis(tropp^{Ph})}]$^+$, is shown in Fig. 2 and reveals it to be penta co-ordinated. The co-ordination sphere corresponds to a trigonal bipyramid (tbp) as is expected for a d^8 valence electron configurated metal centre and a graphical sketch is given in the end of Scheme 4.

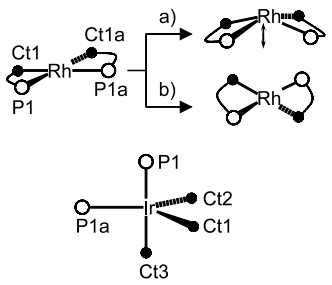

Scheme 4. Schematic depiction of the co-ordination spheres around the metal centres in the complex cations of **15** and **16**. The phosphorus atoms are represented as white circles, the centroids Ct1(C4=C5), Ct1a(C4a=C5a) of the co-ordinated olefin units in **15** and Ct1(C4=C5), Ct2(C23=C30), and Ct3(C26=C27) in **16** as black circles. Rh–Ct1 2.226 Å, Rh–Ct1a 2.212 Å; Ir–Ct1 2.122 Å, Ir–Ct2 2.072 Å, Ir–Ct1 2.218 Å.

The P1 and the centroid Ct3 of the C23=C30 bond take the axial positions [P1–Ir–Ct3 174.0°] and the P1a, the centroid Ct1 of the C4=C5 bond, and the centroid Ct2 of the C26=C27 bond occupy the equatorial positions [P1a–Ir–Ct1 110.3°, Ct1–Ir–Ct2 128.6°, Ct2–Ir–P1a 120.6°]. To our knowledge, this is the first structurally characterised example of a complex with tbp structure, in which an olefin and phosphanyl group, reside in the axial positions. The length of the axial Ir–P1 bond [2.278(1) Å] is very similar to other [Ir(tropp)$_2$X] complexes with a tbp structure [19] and also does not differ much from M–P lengths in the tetra co-ordinated [M(tropp)$_2$] species [1–3,5] (by Δ ca. + 0.05 Å compared with **15** for example). However, the equatorial Ir–P1a bond [2.401(1) Å] is unusually long. The Ir–C distances to the olefins in equatorial position lie in the expected range from 2.175(5) Å (Ir–C23) to

Table 1
Selected bond lengths (Å) and angles (°) for structure **15**

Rh(1)–P(1)	2.208(2)	P(1)–Rh(1)–P(1a)	80.23(9)
Rh(1)–P(1a)	2.227(2)	P(1)–Rh(1)–C(5)	92.3(2)
Rh(1)–C(4)	2.36(1)	P(1a)–Rh(1)–C(5)	156.3(3)
Rh(1)–C(5)	2.31(1)	P(1)–Rh(1)–C(5A)	145.4(3)
Rh(1)–C(4A)	2.331(9)	P(1a)–Rh(1)–C(5A)	89.8(3)
Rh(1)–C(5A)	2.327(9)	C(5)–Rh(1)–C(5A)	83.7(4)
C(4A)–C(5A)	1.36(2)	P(1)–Rh(1)–C(4A)	167.2(3)
C(4)–C(5)	1.38(2)	P(1a)–Rh(1)–C(4A)	87.0(3)
P(1)–C(1)	1.85(1)	C(5)–Rh(1)–C(4A)	99.8(3)
P(1)–C(16)	1.821(7)	C(5A)–Rh(1)–C(4A)	34.0(4)
P(1)–C(22)	1.87(1)	P(1)–Rh(1)–C(4)	85.6(2)
P(1A)–C(1A)	1.85(1)	P(1a)–Rh(1)–C(4)	162.0(3)
P(1A)–C(16A)	1.799(6)	C(5)–Rh(1)–C(4)	34.4(4)
P(1A)–C(22A)	1.85(1)	C(5A)–Rh(1)–C(4)	108.2(4)
C(22A)–C(22)	1.47(2)	C(4A)–Rh(1)–C(4)	106.8(3)

Table 2
Selected bond lengths (Å) and angles (°) for structure **16**

Ir(1)–P(1)	2.278(1)	C(26)–Ir(1)–P(1)	93.8(1)
Ir(1)–P(1A)	2.401(1)	C(27)–Ir(1)–P(1)	89.9(1)
C(4)–C(5)	1.434(7)	C(4)–Ir(1)–P(1)	87.6(1)
C(4A)–C(5A)	1.307(9)	C(5)–Ir(1)–P(1)	88.8(1)
Ir(1)–C(23)	2.303(5)	C(26)–Ir(1)–C(23)	78.3(2)
Ir(1)–C(26)	2.175(5)	C(27)–Ir(1)–C(23)	92.0(2)
Ir(1)–C(27)	2.203(4)	C(4)–Ir(1)–C(23)	78.7(2)
Ir(1)–C(30)	2.343(4)	C(5)–Ir(1)–C(23)	85.4(2)
Ir(1)–C(4)	2.228(5)	P(1)–Ir(1)–C(23)	163.9(1)
Ir(1)–C(5)	2.252(4)	C(26)–Ir(1)–C(30)	84.9(2)
P(1)–C(1)	1.859(6)	C(27)–Ir(1)–C(30)	76.8(2)
P(1)–C(16)	1.861(6)	C(4)–Ir(1)–C(30)	112.5(2)
P(1)–C(22)	1.827(5)	C(5)–Ir(1)–C(30)	107.8(2)
P(1A)–C(1A)	1.913(5)	P(1)–Ir(1)–C(30)	159.9(1)
P(1A)–C(16A)	1.821(6)	C(23)–Ir(1)–C(30)	34.5(2)
P(1A)–C(22A)	1.833(5)	C(26)–Ir(1)–P(1A)	139.4(1)
C(22)–C(22A)	1.522(7)	C(27)–Ir(1)–P(1A)	101.9(1)
		C(4)–Ir(1)–P(1A)	129.0(1)
		C(5)–Ir(1)–P(1A)	92.2(1)
		P(1)–Ir(1)–P(1A)	83.9(4)
		C(23)–Ir(1)–P(1A)	111.3(1)
		C(30)–Ir(1)–P(1A)	84.2(1)
		C(26)–Ir(1)–C(27)	37.5(2)
		C(26)–Ir(1)–C(4)	91.2(2)
		C(27)–Ir(1)–C(4)	128.3(2)
		C(26)–Ir(1)–C(5)	128.3(2)
		C(27)–Ir(1)–C(5)	165.6(2)
		C(4)–Ir(1)–C(5)	37.3(2)

2.228(5) Å (Ir–C4) while the axial Ir–C23/30 bonds are significantly longer [2.303(5), 2.343(4) Å, respectively] (see also the distances to the olefin centroids given in the caption of Scheme 4). In contrast to **15**, the five membered IrP_2C_2 heterocycle in **16** has a twist conformation and the CH_2–CH_2 unit [C22–C22a 1.522(7) Å] shows a staggered conformation [torsion angle P1a–C22a–C22–P1 −44°].

The olefin unit of the tropp ligand, which binds via P1a to the iridium centre, is turned away from the metal centre. One might assume that a complex like **16** is an intermediate on the reaction pathway for the formation of the tetrachelate complex **15**. Although, it is well known that penta co-ordinated complexes of rhodium are much less stable than for iridium, the reluctance of **16** to give up the co-ordination to the remaining cod ligand and to form the desired tetra co-ordinated $[Ir\{R,S\text{-bis}(tropp^{Ph})\}]^+$ complex is somewhat surprising.

4. Electrochemical investigations

The effect of strain energy imposed by the ligand on the properties of a transition metal complex is an important issue in organometallic chemistry. As pertinent recent examples one may refer to the *ansa*-effect in metallocenes used for olefin polymerisations [20] and bond activations [21], or to the ring opening polymerisations (ROP) of ansa-ferrocenes to yield organometallic plastics [22]. The '*wide bite angle*'-effect caused by rigid chelating diphosphanes in transition metal catalysed reactions [23], or, on the contrary, effects evoked by narrow bite angles in four-membered heterocycles like metalladiphosphetanes, $[M(\eta^2\text{-}R_2PCH_2PR_2]$ [24], may also be cited in this context. On the other hand, it was demonstrated that cyclic organometallics, such as metallacyclobutanes, do are much less strained that was a priori assumed [25]. While in most of these studies, strain effects were correlated with reactivity, thermodynamic data of strained organometallic molecules seem to be scarce. Indeed, one can anticipate that in comparison to classical strained organic molecules, less strain energy can be loaded into an organometallic species. Especially for M–L type complexes (L stands for a neutral two electron donor) this may become difficult, because of the relatively weak M–L binding energies. Hence, too much strain will provoke bond fission and in a simple case a larger heterocyclic binuclear complex may form at the expense of a small and strained mono-nuclear complex (of course the entropy loss has to be overcome in this reaction). This means, that the energy differences between comparable strained and unstrained molecules are presumably quite small and hence difficult to measure. In this respect, electrochemical data may be a very valuable tool and thermodynamic relations between the redox active species can be easily extracted from cyclic voltammograms, provided the redox waves are at least quasi-reversible.

In contrast to the complexes $[Rh(tropp^{ph})_2]^+$ **1** and $[Rh(^{me}tropp^{ph})_2]^+$ **17** (Scheme 1), the $[Rh\{R,S\text{-bis}(tropp^{Ph})\}]^+$ complex cation of **15** could not be reversibly reduced in CH_2Cl_2 or acetonitrile as solvents under our conditions (scan rates 100 to −5000 mV s^{-1}, $T = -30$–20 °C). However, in THF as solvent quasi-reversible redox waves were obtained (Fig. 3) which allow the determination of the redox potentials of the couples $[Rh\{R,S\text{-bis}(tropp^{Ph})\}]^+/[Rh\{R,S\text{-}$

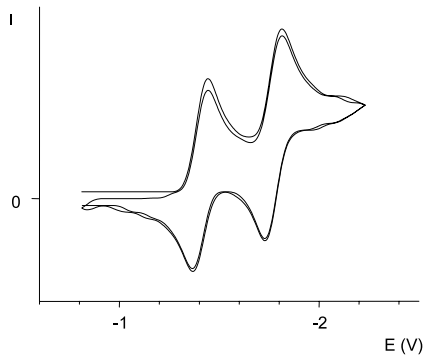

Fig. 3. Cyclic voltammogram of **15** in THF, $v = 100$ mV s^{-1}, $T = 20$ °C.

Table 3
Half-wave peak potentials $E^1_{1/2}$, $E^2_{1/2}$ and potential difference $\Delta E = E^1_{1/2} - E^2_{1/2}$ of **15** **1**, **7** and $[Rh(tropp^{cyc})_2]^+$ vs. [Ag/AgCl] at a scan rates, $v = 100$ mV s^{-1}

	$E^1_{1/2}$ (V)	$E^2_{1/2}$ (V)	ΔE (V)
15	−1.405	−1.772	0.367
1	−0.917	−1.308	0.391
7	−0.882	−1.298	0.416
$[Rh(tropp^{cyc})_2]^+$	−1.189	−1.532	0.343

Working electrode: Pt-wire; electrolyte: THF–0.1 M n-Bu_4NPF_6; $T = 20$ °C.

bis(tropp^{Ph})}]^0 and [Rh{*R*,*S*-bis(tropp^{Ph})}]^0/[Rh{*R*,*S*-bis(tropp^{Ph})}]$^{-1}$.

The half-wave peak potentials $E^1_{1/2}$ and $E^2_{1/2}$ obtained for a scan rate $v = 100$ mV s^{-1} are listed in Table 3. For comparison, the values for **1**, **7** and the P–alkyl substituted complex $[Rh(tropp^{cyc})_2]^+$ (cyc = cyclohexyl [17]) are included.

In contrast to **1** and **7**, the cation [Rh{*R*,*S*-bis(tropp^{Ph})}]$^+$ of **15** is reduced at a potential about 500 mV more negative which corresponds to an energy difference $\Delta(\Delta G°)$ of about 50 kJ mol^{-1}. Not only substitution of electron withdrawing aryl for electron donating alkyl groups on the phosphorus centres account for this relatively large shift. The first redox potential of the complex $[Rh(tropp^{cyc})_2]^+$, in which all P–phenyl groups in the tropp ligand have been replaced by cyclohexyl groups, is only shifted by 290 mV [$\Delta(\Delta G°) = 28$ kJ] to more negative potentials. If we assume that a shift of about 200 mV to more negative potentials is due to an electronic effect caused by replacing one phenyl group for one alkyl group in each tropp unit, there still remains a difference of about 300 mV. Hence, relative to **1** and **7**, the redox couple $[15]^+/[15]^0$ is at least 30 kJ mol^{-1} higher in energy which we attribute to strain in the ligand system. Note, that the potential difference $\Delta E = E^1_{1/2} - E^2_{1/2}$between both redox steps does not change very much for **15**, **1**, **7** and $[Rh(tropp^{cyc})_2]^+$ [min. $\Delta(\Delta G°) = 33$ kJ mol^{-1} for $[Rh(tropp^{cyc})_2]^0/[Rh(tropp^{cyc})_2]^{-1}$; max. $\Delta(\Delta G°) = 40$ kJ mol^{-1} for $[7]^0/[7]^{-1}$]. Therefore, we assume that this extra-energy of ≥ 30 kJ mol^{-1} is build up when the cation [Rh{*R*,*S*-bis(tropp^{Ph})}]$^+$ is reduced to the rhodium(0) complex. The irreversibility of the reductions in acetonitrile or CH_2Cl_2 as solvent, indicate a high reactivity of **15** which is under current investigation.

5. Experimental

5.1. General considerations

All manipulations were performed under dry argon atmosphere. Solvents were distilled from appropriate drying agents.

5.2. Cyclovoltammetry

The electrochemical investigations were performed on an apparatus designed by Heinze et al. [26]. Working electrode: planar platinum electrode (approx. surface area 0.785 mm^2); reference electrode: silver; counterelectrode, platinum wire; tetrahydrofuran, methylene chloride or acetonitrile as solvent. At the end of each measurement, ferrocene was added as internal standard for calibration (+0.352 V vs. Ag/AgCl).

5.3. NMR

Bruker DPX Avance Series 250–300 MHz. ^{1}H- and ^{13}C-chemical shifts are calibrated against the solvent signal ($CDCl_3$, ^{1}H-NMR: 7.27 ppm; ^{13}C-NMR: 77.23 ppm; CD_2Cl_2, ^{1}H-NMR: 5.32 ppm; ^{13}C-NMR: 54.00 ppm). ^{31}P chemical shifts are calibrated against 85% H_3PO_4 as external standard.

5.4. X-ray crystallographic analyses

Single crystals of **15** or **16** were obtained by slow diffusion of *n*-hexane into a concentrated methylene chloride solution. The crystallographic data for **15** and **16** were collected on a Siemens SMART PLATFORM with CCD Detector and are listed in Table 4.

The structures of **15** and **16** were solved by using direct methods. The data sets were refined against the full matrix (vs. F^2) with SHELXTL (Version 5.0) [27]. Non-hydrogen atoms were treated anisotropically, hydrogen atoms were refined on calculated positions using the riding model. For the structure **15** the PF_6 anion was refined isotropically as rigid group. The phenyl-rings at the phosphorus atoms were partially disordered. Crystals of **16** contained two non-coordinating dichloromethane solvent molecules, which were as the CF_3SO_3 counter anion refined with anisotropic temperature factors. An empirical absorption-correction was performed using SADABS. The plots shown in Figs. 1 and 2 were produced by the PLUTO program.

5.5. Syntheses

1,2-bis(phenylphosphano)ethane was prepared following a literature known procedure [15].

5.5.1. Synthesis of the 1,2-[(5H-dibenzo[a,d]-cyclohepten-5-yl)phenylphosphano]ethanes R,S-11 and R,R-/S,S-12, [bis(tropp^{Ph})]

A solution of 1,2-bis(phenylphosphano)ethane (**9**, 1.2 g, 5 mmol) in toluene (50 ml) was added to a solution of 5-chloro-5*H*-dibenzo[a,d]cycloheptene (**10**, 3.5 g, 10

mmol) in toluene (50 ml) at room temperature (r.t.), leading to the precipitation of the hydrophosphonium salt $[\{(trop)PhHPCH_2\}_2]^{2+}$ $2Cl^-$, as a white solid. After stirring for 1 h at r.t., the reaction mixture was refluxed for 30 min. After cooling to r.t., a 1 M solution of potassium carbonate was added and the reaction mixture was refluxed until the organic phase became yellow. The organic layer was then separated and dried over $CaCO_3$. The colourless *meso* compound *R,S*-**11** crystallised from the toluene phase upon cooling to −20 °C (1.23 g, 67%). The racemic mixture of *R,R*-/*S,S*-**12** was subsequently crystallised from a mixture of toluene–acetonitrile (0.61 g, 33%) and contained about 5–8% *R,S*-**11**. Total yield (1.84 g, 60%).

R,S-**11**: melting point (m.p.) 254 °C. MS: $m/z =$ 191.2 [trop, 100%], 435.2 [M-trop, 14%]. ^{31}P-NMR ($CDCl_3$): $\delta = -16.52$, s. ^{1}H-NMR ($CDCl_3$): $\delta = 1.16$ (m, PCH_2CH_2P, 4H), 3.94 (m, C*H*P, 2H), 6.34 (d, $^3J_{HH} = 7.5$ Hz, =C*H*, 2H), 6.85–7.26 (m, =C*H*, 2H, and CH_{ar}, 26H). ^{13}C-NMR ($CDCl_3$): $\delta = 25.1$ (m, PCH_2CH_2P), 61.1 (m, $^1J_{PC} + {}^2J_{PC} = 18.5$ Hz, *C*HP), 127.7 (m, =*C*H), 127.9, 128.6, 129.6, 129.7, 129.9, 130.6, 131.1, 131.3, 131.6, 131.8, 132.9, 133.3, 134.1, 134.7 (m, =*C*H, 1C, and CH_{ar},13C), 136.7 (m, C_{quat}), 136.9 (m, C_{quat}), 139.5 (m, $^1J_{PC} + {}^4J_{PC} = 20.9$ Hz, PC_{quat}), 139.8 (m, C_{quat}), 140.3 (m, C_{quat}).

R,R-/*S,S*-**12**: m.p. 220 °C. ^{31}P-NMR ($CDCl_3$): $\delta = -18.41$, s. ^{1}H-NMR ($CDCl_3$): $\delta = 1.27$ (m, PCH_2CH_2P, 4H), 3.90 (m, C*H*P, 2H), 6.27 (d, $^3J_{HH} =$ 7.5 Hz, =C*H*, 2H), 6.65–7.25 (m, =C*H*, 2H, and CH_{ar}, 26H). ^{13}C-NMR ($CDCl_3$): $\delta = 22.2$ (m, PCH_2CH_2P), 59.4 (m, $^1J_{PC} + {}^2J_{PC} = 16.7$ Hz, *C*HP), 125.8–132.9 (m, =*C*H, 2C, and CH_{ar}, 13C), 133.9 (m, C_{quat}), 136.6 (m, C_{quat}), 137.7 (m, C_{quat}), 139.1 (m, C_{quat}).

Table 4
Crystallographic data for **15** and **16**

	15	**16**
Empirical formula	$C_{55}H_{52}Cl_4F_3IrO_3P_2S$	$C_{44}H_{36}F_6P_3Rh$
Formula weight	1245.97	874.55
Colour	Red	Red
Temperature (K)	233(2)	293(2) K
Wavelength (Å)		0.71073
Crystal system	Orthorhombic	Tetragonal
Space group	$P2_12_12_1$	$P4(1)2(1)2$
Unit cell dimensions		
a (Å)	10.3764(16)	13.42820(10)
b (Å)	19.993(3)	13.42820(10)
c (Å)	24.368(4)	43.3344(2)
V (Å^3)	5055.4(13)	7813.91(9)
Z	4	8
D_{calc} (mg m^{-3})	1.637	1.487
Absorbtion correction	Empirical (SADABS)	
Data collection	Siemens SMART PLATFORM with CCD detector graphite monochromator	
Method	Omega-scans	
Solution by	direct methods	
Absorption coefficient (mm^{-1})	3.013	0.620
F(000)	2496	3552
Crystal size (mm)	$0.62 \times 0.58 \times 0.40$	$0.42 \times 0.34 \times 0.31$
θ range for data collection (°)	1.32–30.54	1.59–23.25
Limiting indices	$-14 \le h \le 14$, $-28 \le k \le 28$, $-34 \le l \le 34$	$-14 \le h \le 14$, $-8 \le k \le 14$, $-48 \le l \le 47$
Reflections collected/unique	59 852/15 257 [$R_{int} = 0.0684$]	37 949/5616 [$R_{int} = 0.0667$]
Completeness to $\theta =$	30.54 (%) 99.9	23.25 (%) 100.0
Max. and min. transmission	0.3787 and 0.2567	0.8310 and 0.7807
Refinement method	Full-matrix least-squares on F^2	
Data/restraints/parameters	15 257/0/622	5616/0/413
Goodness-of-fit on F^2	1.044	1.143
Final *R* indices [$I > 2\sigma(I)$]	$R_1 = 0.0403$, $wR_2 = 0.0890$	$R_1 = 0.0688$, $wR_2 = 0.1831$
R indices (all data)	$R_1 = 0.0582$, $wR_2 = 0.0969$	$R_1 = 0.0744$, $wR_2 = 0.1890$
Largest difference peak and hole (e Å^{-3})	1.505 and −1.543	1.014 and −1.222

5.5.2. Synthesis of {*R,S*-1,2-[(5*H*-dibenzo-[a,d]cyclohepten-5-yl)phenylphosphano]ethane}rhodium hexafluorophosphate (**15**)

Equimolar amounts of *R,S*-1,2-[(5*H*-dibenzo[a,d]-cyclohepten-5-yl)phenylphosphano]ethane, *R,S*-**11**, (254 mg, 0.4 mmol), bis[(chloro)(1,5-cyclooctadiene)-rhodium], **13**, (100 mg, 0.2 mmol) and tallium hexafluorophosphate (141 mg, 0.4 mmol) were dissolved in tetrahydrofuran (20 ml). The resulting reaction mixture was stirred 2 h at r.t. and a red solution and some precipitate were formed. The solvent was evaporated, the residue was re-dissolved in methylene chloride (20 ml), and filtered over Celite. The methylene chloride phase was concentred to 10% of its volume and hexane was added to precipitate the pure complex **15** as red micro-crystalline powder; yield (135 mg, 94%).

^{31}P-NMR (CD_2Cl_2): $\delta = 107.64$ (d, $^1J_{PRh} = 176.8$ Hz). ^{1}H-NMR (CD_2Cl_2): $\delta = 1.52$ (m, CH_2, 2H), 2.40 (m, CH_2, 2H), 4.88 (m, $^2J_{PH} + {}^4J_{PH} = 15.4$ Hz, C*H*P, 2H), 6.67–7.63 (m, =C*H*, 2H, and CH_{ar}, 26H). ^{13}C-NMR (CD_2Cl_2): $\delta = 23.5$ (m, $^1J_{PC} + {}^2J_{PH} = 40.05$ Hz, PCH_2CH_2P), 53.1 (m, $^1J_{PC} + {}^3J_{PC} = 17.3$ Hz, *C*HP), 97.5 (m, =*C*H), 103.1 (m, =*C*H), 127.7 (m, CH_{ar}), 128.1 (m, CH_{ar}), 128.7 (m, CH_{ar}), 129.1 (m, CH_{ar}), 129.4 (m, CH_{ar}), 129.7 (m, CH_{ar}), 130.5 (m, CH_{ar}), 132.1 (m, CH_{ar}), 133.2 (m, C_{quat}), 134.4 (m, C_{quat}), 135.8 (m, C_{quat}), 135.2 (m, C_{quat}).

*5.5.3. Synthesis of {R,S-1,2-[(5H-dibenzo[a,d]-cyclohepten-5-yl)phenylphosphano]ethane} cyclo octadiene iridium trifluoromethanesulfonate (**16**)*

Equimolar amounts of *R,S*-1,2-[(5*H*-dibenzo[a,d]-cyclohepten-5-yl)phenylphosphano]ethane, *R,S*-**11**, (50 mg, 0.08 mmol) and of bis(1,5-cyclooctadien)iridium(I) triflate (44 mg, 0.08 mmol) were dissolved in methylene chloride (20 ml). The resulting orange reaction mixture was stirred 2 h at r.t. The methylene chloride phase was concentred to 10% of its volume and hexane was added to precipitate the pure complex **16** as slightly yellow micro-crystalline powered; yield (57 mg, 88%).

^{31}P-NMR (CD_2Cl_2): $\delta = 12.72$ (s), 66.58 (s).

6. Supplementary material

Crystallographic data (excluding structure factors) for the structures reported in this paper have been deposited with the Cambridge Data Centre as supplementary publication nos. CCDC-171219 (**15**) and CCDC-171218 (**16**). Copies of the data can be obtained free of charge on application to CCDC, 12 Union Road, Cambridge CB21EZ, UK [fax: +44-1223-336033; e-mail: deposit@ccdc.cam.ac.uk or www: http://www.ccdc.cam.ac.uk).

Acknowledgements

This work was supported by the National Science Foundation of Switzerland.

References

[1] J. Thomaier, S. Boulmaâz, H. Schönberg, H. Rüegger, A. Currao, H. Grützmacher, H. Hillebrecht, H. Pritzkow, New J. Chem. 21 (1998) 947.
[2] (a) H. Schönberg, S. Boulmaâz, M. Wörle, L. Liesum, A. Schweiger, H. Grützmacher, Angew. Chem. 109 (1998) 1492;
(b) H. Schönberg, S. Boulmaâz, M. Wörle, L. Liesum, A. Schweiger, H. Grützmacher, Angew. Chem. Int. Ed. Engl. 37 (1998) 1423.
[3] H. Grützmacher, H. Schönberg, S. Boulmaâz, M. Mlakar, S. Deblon, S. Loss, M. Wörle, J. Chem. Soc., Chem. Commun. (1998) 2623.
[4] S. Deblon, L. Liesum, J. Harmer, H. Schönberg, A. Schweiger, H. Grützmacher, Chem. Eur. J. 7 (2001), in press.
[5] S. Deblon, H. Rüegger, H. Schönberg, S. Loss, V. Gramlich, H. Grützmacher, New J. Chem. 23 (2001) 83.
[6] See for example: C.O. Dietrich-Buchecker, J. Guilhem, J.-M. Kern, C. Pascard, J.P. Sauvage, Inorg. Chem. 33 (1994) 3498 and literature cited therein.
[7] See for example: S.A. Jackson, O. Eisenstein, J.D. Martin, A.C. Albeniz, R.H. Crabtree, Organometallics 10 (1991) 3062.
[8] The influence of the distortion of the electronically preferred coordination sphere of a metal centre by the ligand is most prominently exemplified in copper enzymes (entatic state approach). See for example:
[9] G. Pilloni, M. Vecchi, M. Martelli, J. Electroanal. Chem. Interf. Electrochem. 45 (1973) 483.
[10] G. Pilloni, G. Zotti, M. Martelli, Inorg. Chem. 21 (1982) 1284 and literature cited therein.
[11] B.K. Teo, A.P. Ginsberg, K.C. Calabrese, J. Am. Chem. Soc. 98 (1976) 3027.
[12] A.J. Kunin, E.J. Nanni, R. Eisenberg, Inorg. Chem. 24 (1985) 1852.
[13] K.T. Mueller, A.J. Kunin, S. Greiner, T. Henderson, R.W. Kreilick, R. Eisenberg, J. Am. Chem. Soc. 109 (1987) 6313 and literature cited therein.
[14] (a) B. Bogdanović, W. Leitner, C. Six, U. Wilczok, K. Wittmann, Angew. Chem. 109 (1997) 518;
(b) B. Bogdanović, W. Leitner, C. Six, U. Wilczok, K. Wittmann, Angew. Chem. Int. Ed. Engl. 36 (1997) 500.
[15] J. Dogan, J.B. Schulte, G.F. Swiegers, S.B. Wild, J. Org. Chem. 65 (2000) 951.
[16] If the literature reported diastereomer ratio for bis(phosphane) **9** (30% meso and 70% racemic) is correct [15], the reaction with tropylidenyl chloride **10** seems to be quite stereoselective, since this ratio is reversed.
[17] The *trans*-isomers of rhodium tropp complexes show ^{13}C resonances for the co-ordinated olefins which are shifted to lower frequencies ($\Delta\delta \approx 10$–20) than in their corresponding *cis*-isomers: S. Deblon, ETH-Dissertation Nr. 13920 (2000).
[18] A.G. Orpen, L. Brammer, F.H. Allen, O. Kennard, D.G. Watson, R. Taylor, J. Chem. Soc. (1989) S1.
[19] C. Böhler, N. Avarvari, H. Schönberg, M. Wörle, H. Rüegger, H. Grützmacher, Helv. Chim. Acta 84 (2001) 3127.
[20] H.H. Brintzinger, D. Fischer, R. Mülhaupt, B. Rieger, R.M. Waymouth, Angew. Chem. Int. Ed. Engl. 34 (1995) 1143.
[21] For a recent reference on the ansa-effect on C–H and C–C bond activation see: D. Churchill, J.H. Shin, T. Hascall, J.M. Hahn, B.M. Bridgewater, G. Parkin, Organometallics 18 (1999) 2403; and literature cited therein.
[22] I. Manners, J. Chem. Soc., Chem. Commun. (1999) 857.
[23] P.W.N.M. van Leeuwen, P.C.J. Kamer, J.N.H. Reek, P. Dierkes, Chem. Rev. 100 (2000) 2741.
[24] For a recent example see: H. Urtel, C. Meier, F. Eisenträger, F. Rominger, J.P. Joschek, P. Hofmann, Angew. Chem. Int. Ed. Engl. 40 (2001) 781, and literature cited therein.
[25] S.S. Moore, R. DiCosimo, A.F. Sowinski, G.M. Whitesides, J. Am. Chem. Soc. 103 (1981) 948.
[26] K. Hinkelman, J. Heinze, H.T. Schacht, J.S. Field, H. Vahrenkamp, J. Am. Chem. Soc. 111 (1989) 5078.
[27] (a) G.M. Sheldrick, Acta Crystallogr. Sect. A 46 (1990) 467;
(b) G.M. Sheldrick, SHELX 97; Universtität Göttingen, Göttingen, Germany, 1997.